

**Disordered quantum spin chains with long-range antiferromagnetic interactions**

N. Moure\*

*Department of Physics and Astronomy, University of Southern California, Los Angeles, California 90089-0484, USA*

Hyun-Yong Lee†

*Institute for Solid State Physics, University of Tokyo, Kashiwa, Chiba 277-8581, Japan*

S. Haas‡

*Department of Physics and Astronomy, University of Southern California, Los Angeles, California 90089-0484, USA  
and Department of Physics and Earth Sciences, School of Engineering and Science, Jacobs University Bremen, Bremen 28759, Germany*

R. N. Bhatt§

*Department of Electrical Engineering, Princeton University, Princeton, New Jersey 08544, USA*

S. Kettemann||

*Department of Physics and Earth Sciences, School of Engineering and Science, Jacobs University Bremen, Bremen 28759, Germany  
and Division of Advanced Materials Science, Pohang University of Science and Technology (POSTECH), Pohang 790-784, South Korea*

(Received 14 September 2017; revised manuscript received 23 November 2017; published 29 January 2018)

We investigate the magnetic susceptibility  $\chi(T)$  of quantum spin chains of  $N = 1280$  spins with power-law long-range antiferromagnetic couplings as a function of their spatial decay exponent  $\alpha$  and cutoff length  $\xi$ . The calculations are based on the strong disorder renormalization method which is used to obtain the temperature dependence of  $\chi(T)$  and distribution functions of couplings at each renormalization step. For the case with only algebraic decay ( $\xi = \infty$ ) we find a crossover at  $\alpha^* = 1.066$  between a phase with a divergent low-temperature susceptibility  $\chi(T \rightarrow 0)$  for  $\alpha > \alpha^*$  to a phase with a vanishing  $\chi(T \rightarrow 0)$  for  $\alpha < \alpha^*$ . For finite cutoff lengths  $\xi$ , this crossover occurs at a smaller  $\alpha^*(\xi)$ . Additionally, we study the localization of spin excitations for  $\xi = \infty$  by evaluating the distribution function of excitation energies, and we find a delocalization transition that coincides with the opening of the pseudogap at  $\alpha_c = \alpha^*$ .

DOI: [10.1103/PhysRevB.97.014206](https://doi.org/10.1103/PhysRevB.97.014206)**I. INTRODUCTION**

Long-range interactions between local quantum degrees of freedom, such as spins, are ubiquitous in real materials, such as metals with magnetic impurities, doped semiconductors, and glassy systems. In particular, the magnetic susceptibility of doped semiconductors such as P-doped Si is known to diverge at low temperature with an anomalous power law [1], which is evidence for local magnetic moments, formed in localized states [2–5], that are positioned randomly, and are coupled by exchange interactions [6–9], as illustrated in Fig. 1. At low dopant density  $n_D$  these magnetic moments are coupled weakly by the antiferromagnetic exchange interaction  $J$  between the hydrogenlike dopant levels [9,10]. For  $n_D \ll 1/a_B^3$ , where  $a_B$  is the Bohr radius of the dopants, the magnetic susceptibility is observed to follow the Curie law  $\chi \sim n_D/T$  of free magnetic moments [9,11,12]. However,

as  $n_D$  is increased, the magnetic susceptibility diverges as  $\chi \sim T^{-\alpha_m}$  with a decreasing anomalous power  $\alpha_m(n_D) < 1$ . This has been identified as being a consequence of a random distribution of exchange couplings due to the random positions of dopants [13,14]. In Ref. [6] it was argued that such random antiferromagnetically coupled  $S = 1/2$  spins form a ground state of hierarchically coupled singlets, the random singlet phase. The random distribution of excitation energies leads to a temperature-dependent concentration of free magnetic moments  $n_{FM}(T)$ , resulting in an anomalous power  $\alpha_m < 1$ .

With increasing doping concentration, the density of magnetic moments  $n_{FM}$  is observed to decrease. Both magnetic susceptibility and specific heat measurements indicate a finite density  $n_{FM}$  at the metal-insulator transition and deep into the metallic phase [1].

On the metallic side of the transition, the indirect exchange interaction  $J_{ij}$  between the magnetic moments becomes long ranged, mediated by the itinerant electrons [15]. The typical value of this Ruderman-Kittel-Kasuya-Yosida (RKKY) coupling  $J_{ij}$  decays with a power law with exponent  $\alpha = d$ , oscillating in sign with a period equal to the Fermi wavelength  $\lambda_F$ . Its amplitude is widely, log-normally distributed [16]. Thus, aiming to get a better understanding of the magnetic properties of doped semiconductors, we consider the Hamiltonian of  $N$

\* mouregom@usc.edu

† hyunyong.rhee@gmail.com

‡ shaas@usc.edu

§ ravin@exchange.princeton.edu

|| s.kettemann@jacobs-university.de

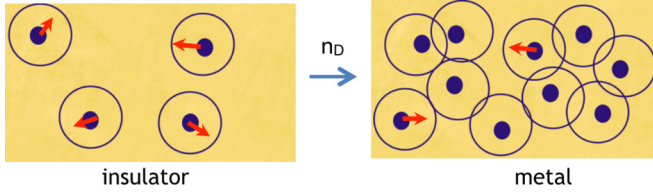


FIG. 1. Left: Sketch of electronic orbitals at low doping concentration  $n_D$ . All states are localized and magnetic, as indicated by red arrows. Right: At larger  $n_D$ , states at Fermi energy are delocalized, coexisting with localized magnetic states.

long-range interacting  $S = 1/2$  spins,

$$H = \sum_{i \neq j} J_{ij}^x (S_i^x S_j^x + S_i^y S_j^y) + J_{ij}^z S_i^z S_j^z, \quad (1)$$

randomly placed on a periodic lattice of length  $L$  and lattice spacing  $a$  using a uniform distribution. The couplings between all pairs of sites  $i, j$  are taken to be antiferromagnetic, decaying as

$$J_{ij}^{x,z} = J_0^{x,z} |\mathbf{r}_i - \mathbf{r}_j| a^{-\alpha} \exp(-|\mathbf{r}_i - \mathbf{r}_j|/\xi), \quad (2)$$

cut off exponentially by length scale  $\xi$ , allowing us to tune between the limit of short-ranged coupled spins for  $\xi \rightarrow L/N^{1/d}$ , and long-range couplings as  $\xi \rightarrow \infty$  [17]. It is worth noting that the initial probability distribution of  $J_{ij}^{x,z}$  depends directly on  $\alpha$  and  $\xi$  by virtue of Eq. (2), together with the fact that the spin positions  $\mathbf{r}_i$  are random.

Based on Eq. (1), the situation in three-dimensional doped semiconductors for experimentally accessible temperatures has been at least semiquantitatively explained [6,9,18,19]. However, ferromagnetic bonds are created in three dimensions at intermediate renormalization steps [6,20], leading to the possibility of new fixed points, and making the asymptotic low-energy and low-temperature behavior a challenging open problem.

Here, we focus on the study of random spin chains with long-range interactions modeled by Eq. (1). From a numerical perspective, one-dimensional models offer the possibility of exploring larger length scales, and therefore to get more accurate asymptotic behavior. From a theoretical perspective, one-dimensional models with power-law hopping [21,22], as well as power-law correlated disorder [23,24], are interesting since they exhibit an Anderson localization-delocalization transition for noninteracting electrons, which has critical properties quite similar to the ones observed in three-dimensional Anderson models [25,26]. Thus, we can expect a delocalization transition in random spin chains with long-range interactions at a critical power  $\alpha_c$  [27].

## II. MAGNETIC SUSCEPTIBILITY

The magnetic susceptibility at low temperatures is determined by the concentration of free paramagnetic moments  $n_{\text{FM}}(T)$  (we set  $k_B = 1$ ) [6],

$$\chi(T) \propto \frac{n_{\text{FM}}(T)}{T} = \frac{n_M}{T} \int_0^T d\epsilon \rho(\epsilon), \quad (3)$$

where  $n_M$  is the total density of magnetic moments in the chain, and  $\rho(\epsilon)$  the density of states of spin excitations with energy  $\epsilon$ .

In order to compute  $n_{\text{FM}}(T)$  numerically, we apply the strong-disorder renormalization group (SDRG) procedure [6,28,29], choosing the pair with largest coupling  $(l, m)$  which in its ground state forms a singlet. Taking the expectation value of the Hamiltonian in that singlet state and performing second-order perturbation theory in the coupling between all spins and the spins of that singlet pair [6,20,28–32], we obtain renormalized couplings between spins  $(i, j)$  [27],

$$(J_{ij}^x)' = J_{ij}^x - \frac{(J_{il}^x - J_{im}^x)(J_{lj}^x - J_{mj}^x)}{J_{lm}^x + J_{lm}^z}, \quad (4)$$

$$(J_{ij}^z)' = J_{ij}^z - \frac{(J_{il}^z - J_{im}^z)(J_{lj}^z - J_{mj}^z)}{2J_{lm}^x}.$$

We implement the SDRG [31] by iterating these RG rules for each realization of bare coupling parameters until the system has reached the energy  $\Omega = T$ . We then record the number of remaining spins which have not yet formed a singlet, obtaining the density  $n_{\text{FM}}(T)$  [6]. We resort to numerical iteration with a large number ( $\sim 20\,000$ ) of random realizations needed for reliable statistics. Two important aspects were checked during the numerical calculations to ensure that the RG flow dictated by Eq. (4) was consistent throughout. First, we monitored that no ferromagnetic couplings were decimated in any of the realizations computed, a possibility that cannot be easily discarded just by looking at the functional form of the RG rules, which include two differences between couplings in the numerator. Second, we verified that the energy scale  $\Omega$ , corresponding to the biggest coupling at each RG step, consistently decreased during the RG procedure, signaling that the RG flow is not breaking down due to the inclusion of all the other couplings beyond nearest neighbor.

In Fig. 2 we show numerical results for the susceptibility of the long-ranged,  $\xi = \infty$ ,  $XX$ -spin chain. Note that the lowest-temperature scale that can be reached for the finite system size  $L$  is of the order of  $T_{\text{min}} = J_{\text{min}}/k_B = J_0(L/2a)^{-\alpha}$ , which is why the data for different values of  $\alpha$  terminate at different values of  $T/J_0$ . At low temperatures, we can see a power-law behavior, which appears linear on a double-logarithmic scale, consistent with a finite dynamical exponent  $z$ . We note that in each RG step, a fraction  $dn_{\text{FM}}/n_{\text{FM}}(\Omega)$  of the remaining spins at renormalization energy  $\Omega = \max(J)$  are taken away. Since this is due to the formation of a singlet with coupling  $J = \Omega$ , this fraction should equal  $2P(J = \Omega, \Omega)d\Omega$ , leading to the differential equation

$$\frac{dn_{\text{FM}}}{d\Omega} = 2P(J = \Omega, \Omega)n_{\text{FM}}(\Omega), \quad (5)$$

where  $P(J, \Omega)$  is the probability distribution of couplings  $J$  at a given renormalization energy  $\Omega$  [29]. At the infinite randomness fixed point (IRFP) this distribution is known to be given by

$$P(J, \Omega) = (J/\Omega)^{1/\Gamma-1}/(\Gamma\Omega), \quad (6)$$

with  $\Gamma = \ln(\Omega_0/\Omega)$  for initial renormalization energy  $\Omega_0$ . Then, the solution of Eq. (5) is  $n_{\text{FM}}(\Omega) = 1/\ln^2(\Omega_0/\Omega)$ , which yields the IRFP magnetic susceptibility  $\chi(T) \sim 1/[T \ln^2(T)]$  via Eq. (3) [29]. However, if  $\Gamma$  is finite and fixed, the solution of Eq. (5) gives  $n_{\text{FM}}(T) \sim T^{2/\Gamma} = T^{1/z}$ , with the dynamical exponent  $z = \Gamma/2$  [33]. In conjunction with Eq. (3), this

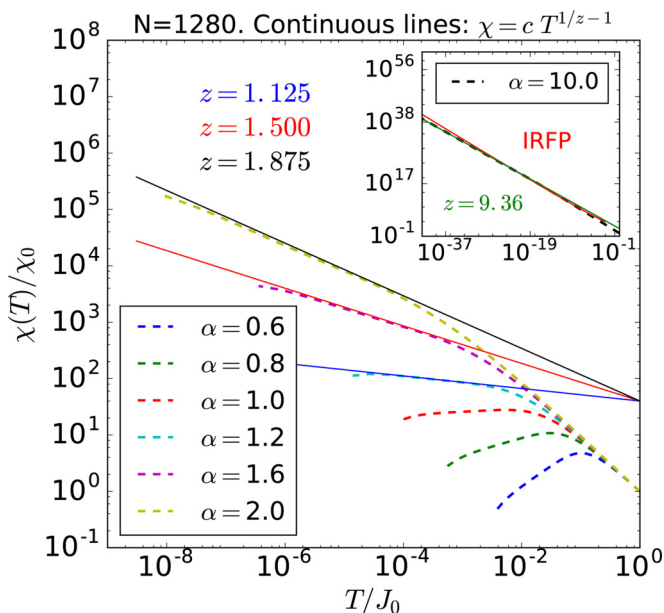


FIG. 2. Magnetic susceptibility, normalized by  $\chi_0 \equiv \chi(T = J_0)$ , for an  $XX$  chain with  $N = 1280$  randomly placed spins, interacting via antiferromagnetic long-range couplings, Eq. (2), chain length  $L/a = 100N$ , and  $\alpha = 0.6, \dots, 2.0$ . The cutoff length is set to  $\xi = \infty$ . Continuous lines: Fits to  $\chi \sim T^{1/z-1}$  with finite  $z$  at low temperatures. Inset: Susceptibility for  $\alpha = 10.0$  along with the power law with  $z = 9.36$  (green line) and the IRFP result (red line).

gives rise to a power-law behavior for the low-temperature susceptibility of the form

$$\chi(T) \sim T^{1/z-1}, \quad (7)$$

consistent with our numerical results shown in Fig. 2 for  $z = z(\alpha)$ , a monotonically increasing function of  $\alpha$  that can be extracted by linear regression fits of the susceptibility in a logarithmic scale (continuous lines). If  $z > 1$ , the magnetic susceptibility diverges as  $T \rightarrow 0$ , with an anomalous power  $\alpha_m = 1 - 1/z < 1$  that also grows with  $\alpha$ . In the region  $z < 1$ , this power becomes negative and we have a vanishing susceptibility at zero temperature, consistent with the formation of a pseudogap in the density of states. A similar behavior has been observed previously in Refs. [6,34]. The crossover value  $z = 1$ , where the susceptibility saturates to a constant, occurs at a given  $\alpha = \alpha^*$ , which from Fig. 2 can be concluded to be somewhere between 1.0 and 1.2. Assuming a linear dependence on  $\alpha$  of the form

$$z = \frac{1-b}{\alpha^*} \alpha + b, \quad (8)$$

we find this crossover value to be  $\alpha^* = 1.066 \pm 0.002$  by a linear regression fit of  $z(\alpha)$ , as shown in Fig. 3 (dashed black line), where the error only includes the fitting uncertainty. All values of  $z$  used for the fit are found by fitting the low-temperature susceptibility curves to Eq. (7) as it is done in Fig. 2 for  $\alpha = 1.2, 1.6$ , and  $2.0$ .

The inset in Fig. 2 displays the susceptibility for  $\alpha = 10.0$ , along with the curve given by Eq. (7) with the value  $z = 9.36$  predicted by Eq. (8), together with the IRFP magnetic susceptibility. We can see clearly a better agreement of the

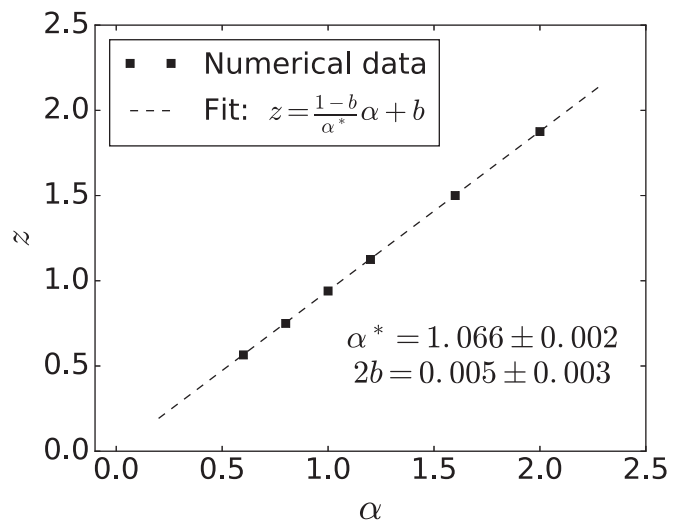


FIG. 3. Dynamical exponent  $z$  extracted by fitting the low-temperature susceptibility in Fig. 2 to Eq. (7) as a function of the power  $\alpha$  (squares). These numerical results are then fit to Eq. (8) (dashed line), which allows us to extract the crossover value  $\alpha^* = 1.066 \pm 0.002$ .

numerical results with the finite  $z$  curve, indicating the flow to a finite  $z$  fixed point and not to the IRFP, as it occurs for nearest-neighbor interactions.

We note that at very large  $\alpha \gg 10$  we find a finite number of free moments even at the smallest renormalization energies which are accessible in the finite spin chain. In our model, spins are randomly placed in a very diluted lattice, a situation in which nearest-neighbor distances bigger than one lattice spacing  $a$  are highly probable. Therefore, at very large values of  $\alpha$ , given the power-law nature of the coupling strengths, one starts with an initial distribution  $P(J)$  heavily weighted near  $J = 0$ , which might explain the above-mentioned residual free moments. A thorough exploration of this important  $\alpha \gg 10$  limit is left for future studies.

### III. WIDTH OF COUPLING DISTRIBUTION FUNCTION

Another way to investigate whether or not there is at finite  $\alpha$  a strong disorder fixed point with a finite dynamical exponent  $z(\alpha)$  or a transition to the IRFP at a specific finite power  $\alpha_{\text{IR}}$  is to numerically inspect the evolution of the width of the coupling probability distribution with the RG flow. At the IRFP, this distribution, according to Eq. (6), gets wider at every RG step, i.e.,  $W = [\langle \ln(J/\Omega_0)^2 \rangle - \langle \ln(J/\Omega_0) \rangle^2]^{1/2} = 2z(\Omega) = \ln(\Omega_0/\Omega)$ , increasing monotonically as  $\Omega$  is lowered during the RG flow. However, as shown in Fig. 4, our system does not follow this trend for  $\alpha \gg 1$  (see the inset). Instead, the width is found to saturate to a constant value after a nonmonotonic transient behavior, which is a strong indication of a finite  $z$  fixed point. It is worth noting that given the large number of couplings present in our system [ $N(N-1)/2$  before any renormalization is performed], we have only picked the largest coupling to every spin  $J_1$  in order to calculate  $P(J)$ , denoting the width of this approximate distribution by  $W_1$ .

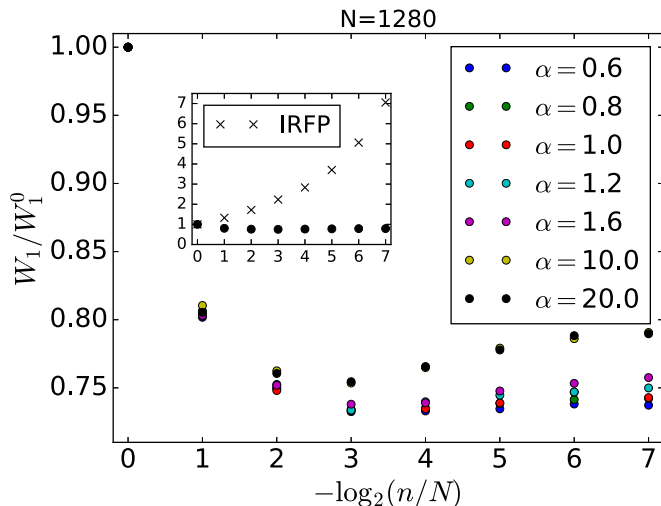


FIG. 4. Width  $W_1$  of the distribution function of nearest-neighbor couplings as a function of the fraction of remaining spins. The negative logarithmic in base two is used to have an equally spaced horizontal variable that grows as the number of spins decreases. All values have been normalized by the width  $W_1^0(\alpha)$  of the initial distribution and the parameters are kept as in Fig. 2. Inset:  $W_1/W_1^0$  for a simple nearest-neighbor model with uniformly distributed couplings (crosses) known to flow to the IRFP. The numerical results for  $\alpha = 20.0$  (black circles) are included for comparison purposes.

#### IV. DISTRIBUTION FUNCTION OF EXCITATION ENERGIES AND THE DELOCALIZATION TRANSITION

In a previous study of the  $\xi = \infty$  limit, we found evidence for a delocalization transition of spin excitations at a critical power  $\alpha_c$  by examining the distribution function of the lowest excitation energy from the ground state of long-range coupled random spin chains ( $N = 128$ ) [27]. At  $\alpha = \alpha_c$ , this gap distribution was observed to coincide with a critical function, separating a phase with localized excitations at large  $\alpha > \alpha_c$ , where the distribution is Poissonian, from a phase with extended excitations at small  $\alpha < \alpha_c$ , where the gap distribution follows the Wigner surmise [35]. Since in our present study we find strong evidence in  $\chi(T)$  that the density of states of spin excitations presents a pseudogap for  $\alpha < \alpha^*$ , we revisit the gap distribution function to check if the delocalization of spin excitations at  $\alpha_c$  coincides with  $\alpha^*$ . Following the procedure carried out in Ref. [27], we now place spins randomly on the sites of a lattice with lattice constant  $a$ , as done in the calculation of the susceptibility above, and study the distribution of excitation energies.

Before proceeding, it is worthwhile to recall the results of Refs. [36,37], where the distribution of excitation gaps  $\epsilon_1$  from the ground state was derived for the random transverse Ising model. Since the probability to find a gap  $\epsilon_1$  is proportional to the number of remaining spins  $N_{\text{FM}} = n_{\text{FM}}(\Omega)L$ , at RG energy  $\Omega$ , the distribution function of the lowest excitation energy  $\epsilon_1$  equal to the energy scale of the last RG step was derived by a scaling argument. Using the same argument for our model, we obtain that the distribution of the excitation energies  $\epsilon_1$  should have the form of a Weibull function [37,38],

$$P_W(\epsilon_1) = \frac{u_0^{1/z} L}{z} \epsilon_1^{1/z-1} \exp[-(u_0 \epsilon_1)^{1/z} L], \quad (9)$$

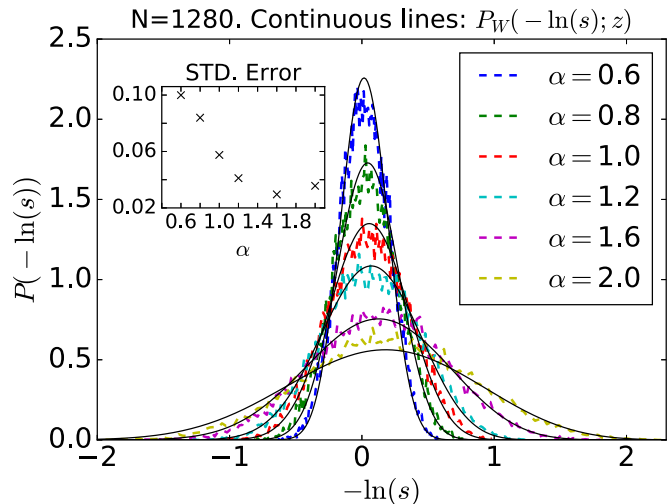


FIG. 5. Distribution of the lowest excitation gap  $\epsilon_1$  scaled by its mean value,  $s = \epsilon_1/\langle\epsilon_1\rangle$ , for  $\xi = \infty$  and  $\alpha = 0.6, 0.8, \dots, 2.0$ . The remaining parameters are as in Fig. 2.

where  $u_0$  is a constant. The average excitation energy scales with system size  $L$  as  $\langle\epsilon_1\rangle = \frac{\Gamma(1+z)}{u_0} L^{-z}$ . Since delocalization causes level repulsion, Eq. (9) yields a delocalization transition when  $z(\alpha) < z_c = 1$ . Thus, if this scaling scheme of the strong disorder RG holds at the delocalization transitions, we conclude that  $z_c = 1 = z^*$ , which means that the first appearance of a pseudogap coincides with the delocalization transition. We note that the eigenvalue statistics of critical random quantum Ising systems with long-range ferromagnetic interactions has recently been found in Refs. [39,40] to follow the Weibull function with finite dynamical exponent  $z = \alpha$  as well.

In Fig. 5 we show the distribution function of the lowest excitation energy  $\epsilon_1$  using the logarithmic variable  $x = -\ln(\epsilon_1/\langle\epsilon_1\rangle)$  in the limit of long-range interaction, i.e.,  $\xi = \infty$ . The continuous black curves correspond to fits to the Weibull distribution in Eq. (9) multiplied by the cutoff function introduced in Ref. [27],  $\exp[c/(x - x_{\text{max}})]$ , which is included in order to account for the fact that at finite size  $L$  with periodic boundary conditions we have a maximum value  $x_{\text{max}} = -\ln[\epsilon_{\text{min}}/\Delta(\alpha)]$  arising from the minimal energy scale  $\epsilon_{\text{min}} = (1/2)J_0(L/6a)^{-\alpha}$ . Here, the factor 6 is included since the numerical data is obtained in the third to last RG step as an effort to minimize the effect of the sharp cutoff due to the finite size of the system. We found  $c = 16$  to work for all fits independent of the value of  $\alpha$ , while  $u_0$  was freely changed for each curve. The fact that the values of  $z(\alpha)$  obtained from the susceptibility data used in conjunction with Eq. (9) can represent fairly well the numerical data for the excitation energy, should not be taken for granted. Equations (7) and (9) are derived using different arguments, and it could well occur that the values of  $z(\alpha)$  shown in Fig. 3 would not fit properly the numerical excitation gap distributions. Since they indeed do, as can be seen in Fig. 5, we can conclude that for  $z < 1$  the existence of the pseudogap in the density of states and the level repulsion dictated by Eq. (9) occur simultaneously. Therefore, we can reuse the results obtained via the analysis of Fig. 3 and confidently claim that, indeed, the delocalization

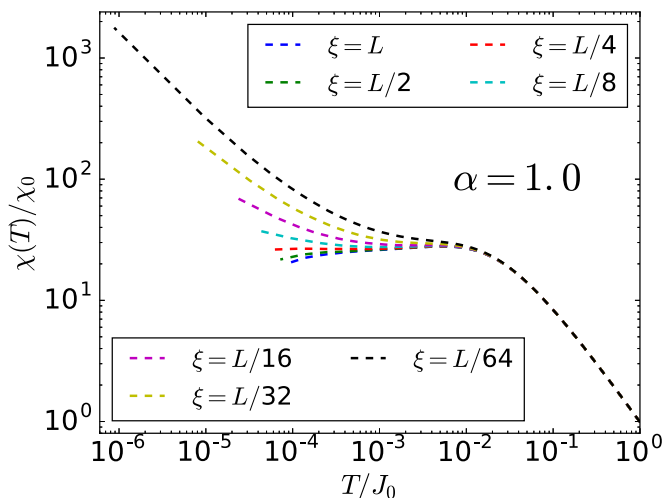


FIG. 6. Log-log plot of the magnetic susceptibility for  $\alpha = d = 1$  and  $\xi/L = 1, 1/2, \dots, 1/64$ . The remaining parameters are kept as in Fig. 2, and the susceptibility is rescaled in the same manner.

transition occurs at the same value at which the pseudogap appears, i.e.,  $\alpha_c = \alpha^* = 1.066 \pm 0.002$ .

As the power  $\alpha = d = 1$  corresponds to the typical decay of the RKKY coupling in a one-dimensional (1D) electron system in the metallic regime, we may conclude from the results in Fig. 2 that the magnetic susceptibility due to the randomly coupled magnetic moments decays to zero in the metallic regime.

### V. EFFECT OF EXPONENTIAL CUTOFF

Turning on a finite cutoff  $\xi$  as caused by the finite electron localization length when the magnetic moments are surrounded by an electronic system, we see in Fig. 6 that the magnetic susceptibility diverges for  $\xi < L/4$ . At low temperatures we observe a power-law behavior indicating a finite  $z$  fixed point. Increasing the cutoff to  $\xi > L/4$ , we observe in Fig. 6 a low-

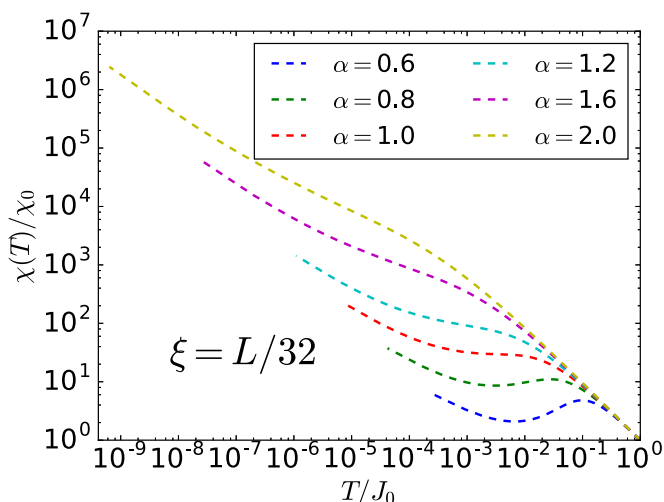


FIG. 7. Logarithmic plot of the susceptibility for a fixed and finite cutoff length  $\xi = L/32$  and  $\alpha = 0.6, 0.8, \dots, 2.0$ . The remaining parameters are kept as in Fig. 2.

temperature suppression of the magnetic susceptibility, clearly demonstrating the opening of a pseudogap as the range of the interaction increases.

For fixed small  $\xi = L/32$ , we observe in Fig. 7 that at sufficiently low temperatures the magnetic susceptibility recovers the power-law divergence consistent with finite  $z > 2$ , after some transient behavior. As expected, due to the presence of a finite  $\xi$ , this divergence is faster for every  $\alpha$  when compared to the pure power-law couplings model, i.e.,  $z(\alpha, \xi = L/32) > z(\alpha, \xi = \infty)$ . In fact, for  $\alpha = 0.6, 0.8$ , and  $1.0$ , we still observe for finite  $\xi$  a divergence in  $\chi(T)$ , in contrast with the results shown in Fig. 2 for  $\xi = \infty$ , where for these values of  $\alpha$  we find  $z(\alpha) < 1$  corresponding to a pseudogap.

### VI. CONCLUSIONS

In conclusion, we derived the temperature dependence of the magnetic susceptibility of quantum spin chains with power-law long-range antiferromagnetic couplings as a function of the exponent  $\alpha$  and the cutoff length  $\xi$ . We identified a crossover between a phase with a divergent low-temperature magnetic susceptibility to a phase with a vanishing low-temperature susceptibility at a critical  $\alpha^*$ . For finite cutoff lengths  $\xi$ , this crossover occurs at smaller values  $\alpha^*(\xi) < \alpha^*$ . We also explored the localization of spin excitations in the limit  $\xi = \infty$ , by computing the distribution functions of renormalized couplings and identified a delocalization transition at  $\alpha_c$ , which turns out to coincide with  $\alpha^*$ .

It is worth noting that the good agreement found between numerical results and both Eqs. (7) and (9) demonstrates the consistency of SDRG and indicates that it continues to be a valid tool to study spin chains when long-range interactions are included. The error induced by all couplings beyond nearest neighbor must yet be quantified. This can be done by adding corrections to the random singlet state generated by SDRG, which is asymptotically exact when only nearest-neighbor interactions are included. These corrections go beyond the SDRG standard framework and we are currently working on their implementation. We leave the findings on this matter for a future publication.

In order to analyze experimental results in doped bulk semiconductors, the study of higher-dimensional random spin systems with long-range couplings is needed. However, in higher dimensions it is known that even if the initial distribution is purely antiferromagnetic, ferromagnetic couplings can be generated upon renormalization [6,20]. This is expected to modify strongly the temperature dependence of the magnetic susceptibility. Furthermore, as the density of itinerant electrons increases with the doping concentration, the indirect exchange coupling competes with the Kondo effect, which screens the local moments with the itinerant electron spins. Indeed, on the metallic side of the transition in P:Si there are indications of Kondo correlations in thermopower measurements [41]. It has been shown that the Kondo temperature  $T_K$  is widely distributed in the vicinity of the Anderson metal-insulator transition (AMIT), which results in a power-law divergence of the magnetic susceptibility [42–46]. Its power  $\alpha_m$  has been related to multifractal correlations, yielding in  $d = 3$  dimensions with the multifractality parameter  $\alpha_0$ ,  $\alpha_m = 2 - \alpha_0/3 = 0.651(0.652, 0.650)$  [46], which happens to be close

to the experimentally observed value [1,10–12]. It remains a challenge to study the effect of the interplay of both the long-range exchange couplings and the Kondo couplings on the low-temperature magnetic properties.

### ACKNOWLEDGMENTS

This research has been supported by DFG KE-15 Collaboration grant. H.Y.L. acknowledges support from MEXT

as Exploratory Challenge on Post-K computer (Frontiers of Basic Science: Challenging the Limits). S.H. acknowledges funding by DOE Grant No. DE-FG02-05ER46240 and would also like to thank the Humboldt Foundation for support. R.N.B. acknowledges support from DOE Grant No. DE-SC0002140, and during the writing of the manuscript, the hospitality of the Aspen Center for Physics. Computation for the work described in this paper was supported by the University of Southern California's Center for High-Performance Computing.

- 
- [1] H. v. Löhneysen, *Adv. Solid State Phys.* **40**, 143 (2000).  
 [2] P. W. Anderson, *Phys. Rev.* **109**, 1492 (1958).  
 [3] P. W. Anderson, in *Nobel Lectures in Physics 1971–1980*, edited by S. Lundqvist (World Scientific, Singapore, 1980), p. 376.  
 [4] N. F. Mott, *J. Phys. Colloq.* **37**, C4-301 (1976).  
 [5] A. M. Finkel'shtein, *JETP Lett.* **46**, 513 (1987).  
 [6] R. N. Bhatt and P. A. Lee, *Phys. Rev. Lett.* **48**, 344 (1982).  
 [7] R. N. Bhatt, *Phys. Scr.* **T14**, 7 (1986).  
 [8] M. Milovanovic, S. Sachdev, and R. N. Bhatt, *Phys. Rev. Lett.* **63**, 82 (1989).  
 [9] K. Andres, R. N. Bhatt, P. Goalwin, T. M. Rice, and R. E. Walstedt, *Phys. Rev. B* **24**, 244 (1981).  
 [10] R. N. Bhatt, M. Paalanen, and S. Sachdev, *J. Phys. Colloq.* **49**, C8-1179 (1988).  
 [11] M. P. Sarachik, A. Roy, M. Turner, M. Levy, D. He, L. L. Isaacs, and R. N. Bhatt, *Phys. Rev. B* **34**, 387 (1986).  
 [12] M. Lakner and H. v. Löhneysen, *Phys. Rev. Lett.* **70**, 3475 (1993).  
 [13] R. N. Bhatt and T. M. Rice, *Philos. Mag. B* **42**, 859 (1980).  
 [14] M. Rosso, *Phys. Rev. Lett.* **44**, 1541 (1980).  
 [15] M. A. Ruderman and C. Kittel, *Phys. Rev.* **96**, 99 (1954); T. Kasuya, *Prog. Theor. Phys.* **16**, 45 (1956); K. Yosida, *Phys. Rev.* **106**, 893 (1957).  
 [16] I. V. Lerner, *Phys. Rev. B* **48**, 9462 (1993).  
 [17] In this work we restrict ourselves to the case of power-law decaying couplings without alternating sign. Inclusion of the sign alternation will likely lead to different fixed points of mixed character, such as discussed in Ref. [20].  
 [18] M. A. Paalanen, J. E. Graebner, R. N. Bhatt, and S. Sachdev, *Phys. Rev. Lett.* **61**, 597 (1988).  
 [19] S. Sachdev, *Phys. Rev. B* **39**, 5297 (1989).  
 [20] E. Westerberg, A. Furusaki, M. Sigrist, and P. A. Lee, *Phys. Rev. B* **55**, 12578 (1997); *Phys. Rev. Lett.* **75**, 4302 (1995).  
 [21] A. D. Mirlin, Y. V. Fyodorov, F.-M. Dittes, J. Quezada, and T. H. Seligman, *Phys. Rev. E* **54**, 3221 (1996).  
 [22] C. Zhou and R. N. Bhatt, *Phys. Rev. B* **68**, 045101 (2003).  
 [23] F. de Moura and M. L. Lyra, *Phys. Rev. Lett.* **81**, 3735 (1998); *Physica A (Amsterdam)* **266**, 465 (1999).  
 [24] F. M. Izrailev and A. A. Krokhin, *Phys. Rev. Lett.* **82**, 4062 (1999).  
 [25] P. A. Lee and T. V. Ramakrishnan, *Rev. Mod. Phys.* **57**, 287 (1985).  
 [26] F. Evers and A. Mirlin, *Rev. Mod. Phys.* **80**, 1355 (2008).  
 [27] N. Moure, S. Haas, and S. Kettemann, *Europhys. Lett.* **111**, 27003 (2015).  
 [28] C. Dasgupta and S.-K. Ma, *Phys. Rev. B* **22**, 1305 (1980).  
 [29] D. S. Fisher, *Phys. Rev. B* **50**, 3799 (1994).  
 [30] D. S. Fisher, *Phys. Rev. Lett.* **69**, 534 (1992).  
 [31] F. Igloi and C. Monthus, *Phys. Rep.* **412**, 277 (2005).  
 [32] E. Yusuf and K. Yang, *Phys. Rev. B* **68**, 024425 (2003).  
 [33] The factor of 2 difference between  $\Gamma$  and  $z$  comes from the factor in Eq. (5) introduced to take into account that at each RG step two sites are being decimated. In the disordered quantum Ising model studied in Ref. [29], this factor does not appear since only one site is decimated, and hence  $\Gamma = z$ .  
 [34] R. Bhatt (unpublished).  
 [35] We note that these fitting functions had to be multiplied by a cutoff distribution of the form  $e^{c/(x-x_{\max})}$  [ $x = -\log(s)$ ], where  $c > 0$ , to account for the finite size of the system giving rise to a minimum excitation energy of the order of  $s_{\min} = (L/2)^{-\alpha} / \Delta$  [ $x_{\max} = -\log(s_{\min})$ ], where  $\Delta \equiv \Delta(\alpha)$  is the average excitation gap.  
 [36] D. S. Fisher and A. P. Young, *Phys. Rev. B* **58**, 9131 (1998).  
 [37] R. Juhász and Y.-C. Lin, F. Igloi, *Phys. Rev. B* **73**, 224206 (2006).  
 [38] A. Papoulis and S. U. Pillai, *Probability, Random Variables, and Stochastic Processes*, 4th ed. (McGraw-Hill, Boston, 2002).  
 [39] R. Juhász, I. A. Kovács, and F. Iglói, *Europhys. Lett.* **107**, 47008 (2014).  
 [40] I. A. Kovács, R. Juhász, and F. Iglói, *Phys. Rev. B* **93**, 184203 (2016).  
 [41] H. G. Schlager and H. v. Löhneysen, *Europhys. Lett.* **40**, 661 (1997).  
 [42] R. N. Bhatt and D. S. Fisher, *Phys. Rev. Lett.* **68**, 3072 (1992).  
 [43] A. Langenfeld and P. Wölfle, *Ann. Phys.* **4**, 43 (1995).  
 [44] V. Dobrosavljevic, T. R. Kirkpatrick, and G. Kotliar, *Phys. Rev. Lett.* **69**, 1113 (1992); E. Miranda, V. Dobrosavljevic, and G. Kotliar, *ibid.* **78**, 290 (1997).  
 [45] P. S. Cornaglia, D. R. Grempel, and C. A. Balseiro, *Phys. Rev. Lett.* **96**, 117209 (2006).  
 [46] S. Kettemann, E. R. Mucciolo, and I. Varga, *Phys. Rev. Lett.* **103**, 126401 (2009); S. Kettemann, E. R. Mucciolo, I. Varga, and K. Slevin, *Phys. Rev. B* **85**, 115112 (2012).